Electronic Supplementary Material (ESI) for Physical Chemistry Chemical Physics.

Supporting Information: Selective solute adsorption and partitioning around single PNIPAM chains

Matej Kanduč,[*,†] Richard Chudoba,[†,‡] Karol Palczynski,[†] Won Kyu Kim,[†] Rafael Roa,[†] and Joachim Dzubiella[*,†,‡]

†Soft Matter and Functional Materials, Helmholtz-Zentrum Berlin für Materialien und Energie, Hahn-Meitner-Platz 1, D-14109 Berlin, Germany
‡Institut für Physik, Humboldt-Universität zu Berlin, Newtonstr. 15, D-12489 Berlin, Germany

E-mail: matej.kanduc@helmholtz-berlin.de; joachim.dzubiella@helmholtz-berlin.de

1. FREE POLYMER CHAIN IN WATER

For the purposes of determining the contour length and the end-to-end distance of a free PNIPAM chain, we perform simulations of an non-replicated PNIPAM chain consisting of $N = 20$ monomer units, solvated by 10,500 water molecules in a cubic simulation box with a size of ~7 nm. The simulations are produced in canonical constant-pressure (NPT) ensemble with a duration of 100–200 ns (of which 10 ns are used for equilibration) at different temperatures.

1.1. Contour length. We define the contour length L_c of the polymer segment as the sum over the distances between adjacent chiral carbon atoms in the backbone (corresponds to the distances between adjacent monomers), $L_\mathrm{c} = \sum_i |\mathbf{r}_{i+1} - \mathbf{r}_i|$. Here, $\mathbf{r}_i$ represent the successive positions of the chiral carbon atoms in the backbone.

The evaluated average distance between adjacent monomers at $T = 300$ K is $\Delta L_\mathrm{c} = 0.266$ and 0.264 nm for isotactic and syndiotactic polymers, respectively. Since the 20-monomers-long non-replicated chains have 19 bonds, this corresponds to the total contour length of $L_\mathrm{c} = 19\Delta L_\mathrm{c} =$ 5.05 and 5.02 nm, respectively. However, in the case when the chains are periodically replicated, as in our study (Fig. 1b), the simulation box contains 20 bonds, which leads to the contour lengths of $L_\mathrm{c} = 20\Delta L_\mathrm{c} = 5.32$ and 5.28 nm, respectively. The contour length depends only insignificantly on temperature.

1.2. Polymer elongation. In the next step, we sample the end-to-end distance $R_\mathrm{ee}(t)$ of the chains, that is, the distance between the terminal chiral carbon atoms (see Fig. S1a). The elongation of the chain λ is in this case defined as the ratio between the average end-to-end distance $\langle R_\mathrm{ee}\rangle$ and the chain's contour length L_c, viz.

$$\lambda = \frac{\langle R_\mathrm{ee}\rangle}{L_\mathrm{c}}. \tag{S1}$$

Figure S1b shows the elongation parameter as a function of temperature for both considered tacticities. In both cases, the chain is considerably extended at lower temperatures and collapses at high temperatures (see Fig. S1a for snapshots). This abrupt change in R_ee is a fingerprint of the coil–globule transition of the PNIPAM polymer, which can, however, deviate from the thermodynamic limit of a long polymer chain or a cross-linked network. Here, due to the finite size of the chain, the transition is much less abrupt than for longer chains. We nevertheless reproduce the experimental trend, where the syndiotactic polymer has higher transition temperature than the isotactic one.[1]

The largest elongation is around $\lambda = 0.75$–0.85, indicated by a blue-shaded stripe in Fig. S1. This interval is an estimate for the maximal elongation of chain sequences in a swollen PNIPAM hydrogel.

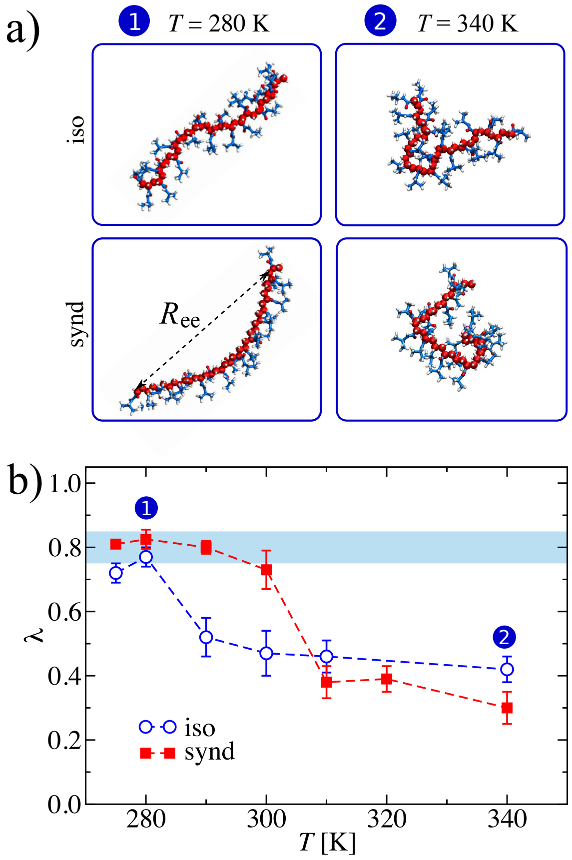

Figure S1: (a) Snapshots of 20-monomers-long PNIPAM chains in water (not shown) in their isotactic (iso) and syndiotactic (synd) variants and at two different temperatures (denoted as 1 and 2 in panel (b)). (b) Elongation λ obtained via Eq. (S1) of 20-monomer long isotactic and syndiotactic chains as a function of temperature.

2. PARTIAL CHARGES IN THE NITRO MOLECULES

In our simulations, we use the OPLS-AA force field for the solutes.[2] However, the partial charges of the nitrophenolate ion, NP^-, are not provided within the force field and have to be determined independently.

As the main focus of our study lies on the aromatic nitro compounds, we perform a verification of the simulation results by an additional set of simulations with alternative force-field parameters. To that end, we independently determine the charge distribution in the aromatic nitro molecules NB and NP^0 based on quantum mechanical calculations, which we describe in the following.

2.1. Evaluation of partial charges. We determine charge distribution in the three studied aromatic nitro molecules (NB, NP^0, and NP^-) based on quantum mechanical calculations using the Gaussian 09 software.[3] We employ the B3LYP functional with the cc-PVTZ basis set using the electrostatic potential fitting method (ESP).[4] The ESP method bridges the gap between the classical coulomb model for the electrostatic potential and the 'accurate' quantum mechanical description, and it is therefore well suited for polar molecules in MD simulations.[5] The point charge calculations are performed in two environments, (i) in vacuum (referred to as QM1) and (ii) in implicit solvent with dielectric constant $\varepsilon = 78.35$ (referred to as QM2). For the latter, we employ the Polarizable Continuum Model (PCM), which performs self-consistent reaction-field calculations based on the integral equation formalism model. See Refs. [3, 6] for more details. The charges are generated from the final structure of a geometry optimization on B3LYP level. The spin multiplicities are all set to 1 (*i.e.*, zero net spin) and the net charges are predefined as 0 in cases of NB and NP^0 and -1 in the case of NP^-.

The partial-charge values of the nitro molecules, rounded to three digits, are shown in Fig. S2. Since the molecules are symmetric with respect to the vertical, the partial charges are equivalent on both sides of the molecule (denoted only once).

Comparing the partial charges in NB and NP^0 provided by the OPLS-AA force field with those obtained by Gaussian, it can be seen that the difference is not significant. The independently evaluated partial charges enable us to compare the results from the original OPLS-AA force field, termed as 'OPLS' parameterization in our text, with the modified force fields containing the partial charges as obtained by the QM calculation (QM1 and QM2). All other model parameters are kept as in the original OPLS-AA force field.

2.2. Force fields for NP^-. Partial charges of the nitrophenolate NP^- ion are not provided within the OPLS-AA force field. Therefore, constructing its model requires resolving the partial charges separately.

In this study, we compare three different approaches for determining the partial charges. All cases are based on quantum-mechanical calculations. The Lennard-Jonnes and the bonded parameters of the molecule are in all cases adopted from the OPLS-AA force field.

a) **Quantum-mechanical (QM1) in vacuum:** In the first approach, we assign the charge distribution obtained from the quantum calculations in vacuum via

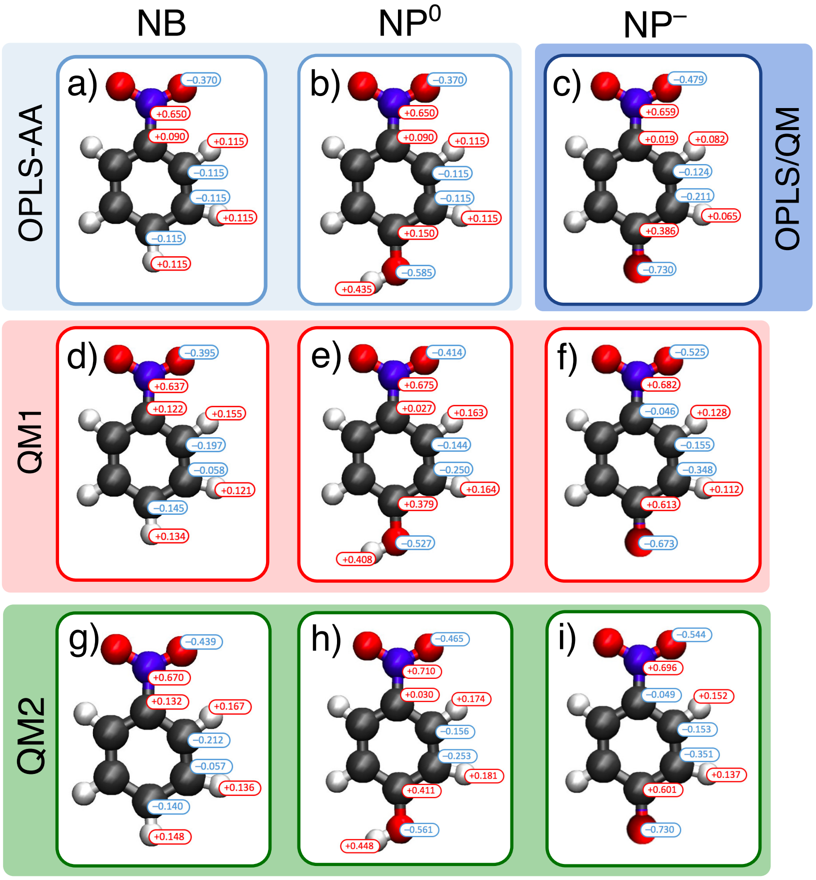

Figure S2: Partial charges of aromatic nitro molecules: nitrobenzene (NB), protonated nitrophenol (NP^0), and deprotonated nitrophenol (NP^-) as provided by the OPLS-AA force field (a, b), evaluated via QM calculations by Gaussian in vacuum (d, e, f) and implicit solvent (h, h, i), and by the combination of the OPLS and QM parameters via Eq. (S2) (c).

Gaussian to the partial charges of NP^- atoms. We refer to this parameterization as 'QM1' parameterization, NP^-(QM1). The results are shown in Fig. S2f.

b) Quantum-mechanical (QM2) in implicit solvent: The second approach, which is similar to QM1, contains an implicit solvent mimicking water environment based on self-consistent reaction-field calculations implemented in Gaussian simulation package, see above. The corresponding results are shown in Fig. S2i.

c) OPLS/QM1 (O/QM1): In the third approach we determine the partial charges of NP^- by a combination of the charge distribution from QM1 and the OPLS-based partial charges of the protonated molecules. The difference between the charge distributions in NP^0(QM1) and NP^-(QM1) as evaluated by Gaussian in vacuum (Figs. S2e and f) gives the information about the charge redistribution upon deprotonation of the hydroxyl group, $NP^0 \to NP^-$. Adding this difference of the partial charges respectively on top of the partial charges of NP^0(O) provided by OPLS-AA, gives a hybrid 'OPLS/QM1' parameterization, which we denote as NP^-(O/QM1). A partial charge of each atom in the NP^-(O/QM1) is thus respectively defined as

$$NP^-(O/QM1) := NP^0(O) - NP^0(QM1) + NP^-(QM1). \tag{S2}$$

A tiny charge of +0.027 that remains left on the phantom site of the removed hydrogen in the OH group we uniformly redistribute throughout the molecule. The obtained partial charges for NP^-(O/QM1) are shown in Fig. S2c.

All three approaches yield quite similar results for the partial charges in NP^{-}. As can be seen, the deprotonated oxygen and its neighboring atoms exhibit a rather neutral but very polar character. The negative excess charge of -1 is namely delocalized throughout the entire molecule, partially absorbed by the nitro group on the other side of the molecule due to its negative mesomeric (–M) effect.

3. ADSORPTION PER CONTOUR LENGTH

The adsorption coefficient Γ', defined via Eq. (4) in the main text, represents the number of adsorbed solutes per longitudinal extension L_z of the chain. An alternative way is to express the adsorption per chain's contour length L_c instead of per L_z. By combining Eqs. (1) and (4) in the main text, the total adsorption expresses as

$$\Gamma = (\lambda\Gamma')\, c_0 L_c. \tag{S3}$$

Thus, the product $\lambda\Gamma'$ corresponds to the adsorption coefficient expressed per contour length.

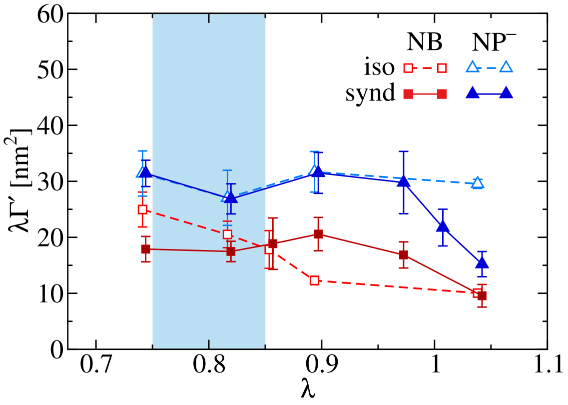

Figure S3: Same plot as in Fig. 4 in the main text, but with the adsorption coefficient Γ' rescaled by the chain elongation λ, which corresponds to the adsorption coefficient expressed per chain's contour length.

As can be seen from Fig. S3 the adsorption coefficient expressed per contour length, $\lambda\Gamma'$, shows less dependency on the elongation than when expressed per longitudinal elongation, Γ' (cf. Fig. 4 in the main text). While NB shows a weak dependence on the elongation λ, NP^{-} shows no significant dependence for a loose chain, $\lambda < 1$. For an overstretched chain ($\lambda > 1$), however, the difference between the isotactic and syndiotactic chains become significant for NP^{-}.

4. CONTACT FRACTIONS

In this section we provide the binding analysis used in Section 3.3 in the main text based on monitoring the distance between the atoms in a solute molecule and the polymer. This method enables a more detailed analysis of adsorption than the integration of RDFs.

4.1. Total residence time. In the course of simulations we measure closest distance between the atoms in a solute and in the PNIPAM chain, as denoted by d_{all} in the example in Fig. S4a.

Figure S4b shows a 10-ns-long trajectory of the closest distance d_{all} between PNIPAM and NP^{-} by a red curve. When the solute molecule approaches the polymer closer than the threshold distance d_0, the solute molecule is considered as bound. The adsorption thus depends on the choice of the threshold value d_0. In our case, we choose the value d_0 such that the adsorption evaluated from the distance measurements equals to the adsorption obtained from integration of RDF, as we will explain in the following.

The total residence time τ_{tot} of a molecule on the chain (*i.e.*, the total time the molecule is bound) in the course of a simulation depends on the simulation box size $L_x \times L_y \times L_z$, as the available space the molecule can explore determines the frequency with which it is revisiting the chain. The ratio between the total residence time τ_{all} and the total simulation time t_{sim} is equal to the ratio between the amount that is adsorbed on the chain, $\Gamma = \Gamma' c_0 L_z$, and the total number of molecules N_{tot} in the system,

$$\frac{\tau_{\text{all}}}{t_{\text{sim}}} = \frac{\Gamma' c_0 L_z}{N_{\text{tot}}}. \tag{S4}$$

The total number of solute molecules, which is in our case $N_{\text{tot}} = 1$, can be written as composed of the adsorbed amount and the amount outside the Gibbs dividing radius R_0 with a bulk concentration c_0,

$$N_{\text{tot}} = \Gamma' c_0 L_z + c_0 (L_x L_y - \pi R_0^2) L_z. \tag{S5}$$

Eliminating c_0 from both above equations, yields

$$\frac{\tau_{\text{all}}}{t_{\text{sim}}} = \frac{\Gamma'}{\Gamma' + L_x L_y - \pi R_0^2}. \tag{S6}$$

Equation (S6) enables us to compute the residence time based on the known adsorption coefficient Γ', which is in our case obtained by integration of RDF. Alternatively, we can determine the residence time τ_{all} as the overall time the molecule approaches the chain closer than the threshold value, $d_{\text{all}} < d_0$. Choosing the threshold value

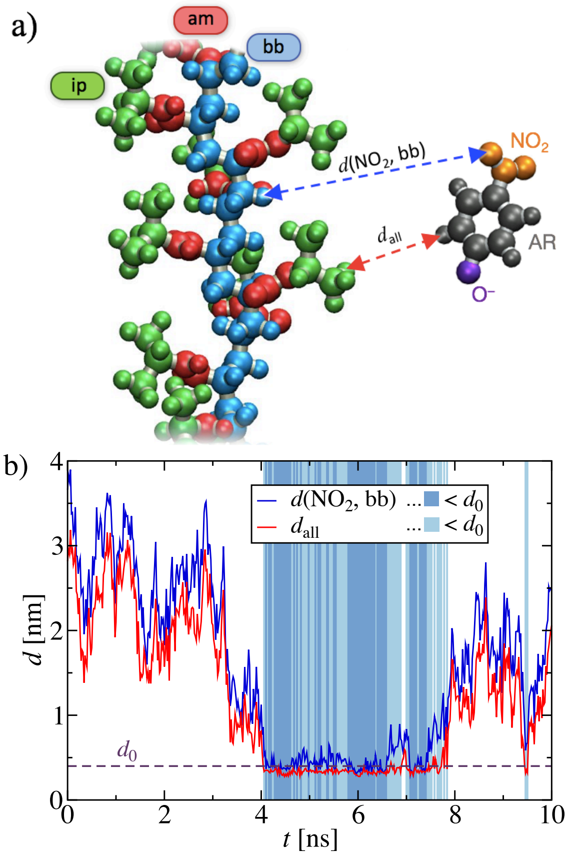

Figure S4: (a) Simulation snapshot (water not shown) of a PNIPAM polymer in the presence of $\mathrm{NP^-}$. Atoms of different groups in the polymer (ip, am, bb) as well as in the $\mathrm{NP^-}$ molecule ($\mathrm{NO_2}$, AR, $\mathrm{O^-}$) are denoted by different colors. The blue arrow shows the closest distance between the nitro group ($\mathrm{NO_2}$) and the backbone (bb), $d(\mathrm{NO_2}, \mathrm{bb})$. The red arrow represents the closest distance between the $\mathrm{NP^-}$ and the polymer, d_{all}. (b) Closest distances $d(\mathrm{NO_2}, \mathrm{bb})$ and d_{all} as a function of time. When the two distances are below the threshold of $d_0 = 0.4$ nm (horizontal dashed line), the two groups and the molecule are considered as bound, respectively. The bound states ($d_{\mathrm{all}} < d_0$) are denoted by blue regions, where the darker shade corresponds to $d(\mathrm{NO_2}, \mathrm{bb}) < d_0$.

$d_0 = 0.4$ nm yields the same τ_{all} for NB as calculated from Eq. (S6). Not surprisingly, the fitted value $d_0 = 0.4$ nm roughly corresponds to the LJ diameter of the carbon atom $\sigma_{\mathrm{LJ}} = 0.35$ nm in the OPLS force field.[2] The shaded regions in Fig. S4b show the instances where $d_{\mathrm{all}} < d_0$ and the molecule is considered as bound.

4.2. Contact fractions. Detailed information on binding can be gained by additionally computing the closest distance $d(X, Y)$ between the group $X \in \{\mathrm{NO_2}, \mathrm{AR}, \mathrm{OH/O^-}\}$ in the solute molecule and the groups $Y \in \{\mathrm{ip}, \mathrm{am}, \mathrm{bb}\}$ in the polymer, as shown in Fig. S4a for the case $X = \mathrm{NO_2}$ and $Y = \mathrm{bb}$.

We assign the groups X and Y as bound at a given moment if they approach a distance that is below the threshold value of $d_0 = 0.4$ nm. This enables us to define a total residence time $\tau(X, Y)$ of the groups X and Y as the cumulative time in the course of the simulation where $d(X, Y) < d_0$. The darker blue shade in Fig. S4b denotes the instances where $d(\mathrm{NO_2}, \mathrm{bb}) < d_0$, that is, where the nitro group is bound to the polymer backbone.

We define the contact fraction of the groups X and Y as the ratio between the residence time $\tau(X, Y)$ of the groups X and Y and the total residence time τ_{all} of the solute to the polymer,

$$\text{contact fraction} = \frac{\tau(X, Y)}{\tau_{\mathrm{all}}}. \tag{S7}$$

The contact fractions for NB, $\mathrm{NP^0}$, and $\mathrm{NP^-}$ are shown in Fig. 6 in the main text.

5. ADSORPTION OF A WEAKLY INTERACTING GAS

We estimate the adsorption coefficient Γ' of solutes on a polymer chain in terms of a virial-expansion approach. In the following approximation, we treat the adsorbed solutes on the surface of the polymer as two dimensional weakly-interacting gas.

A two-dimensional gas of particles interacting with one another in the plane has to order N^2 in a virial expansion the free energy given by[7]

$$F_{\mathrm{2D}}^0 = N k_{\mathrm{B}} T \left(\log \frac{\lambda^3 N}{A\delta} - 1 \right) + \frac{N^2 k_{\mathrm{B}} T B_2^{(\mathrm{2D})}}{A}. \tag{S8}$$

Here, N is the total number of adsorbed particles on the surface of area A, δ is an effective width of the adsorbed layer, and $B_2^{(\mathrm{2D})}$ is the surface second virial coefficient given by

$$B_2^{(\mathrm{2D})} = -\pi \int_0^\infty [\mathrm{e}^{-u(r)/k_{\mathrm{B}} T} - 1] r \mathrm{d}r, \tag{S9}$$

where $u(r)$ is the pair interaction between two particles. In order to describe the particles adsorbed on the surface, we add a term ϵN to account for the effective binding energy,

$$F_{\mathrm{2D}} = F_{\mathrm{2D}}^0 + \epsilon N. \tag{S10}$$

The chemical potential of the adsorbed particles $\mu =$

$(\partial F_{2\mathrm{D}}/\partial N)_{A,T}$ is then

$$\mu = k_\mathrm{B}T \, \log\left(\lambda^3 N/A\delta\right) + 2k_\mathrm{B}TB_2^{(2\mathrm{D})}N/A + \epsilon. \quad \text{(S11)}$$

Equating it with the chemical potential of the surrounding bulk ideal gas $\mu = k_\mathrm{B}T \, \log \lambda^3 c_0$, where c_0 is its density, we obtain

$$N/A = c_0\delta \mathrm{e}^{-\epsilon/k_\mathrm{B}T}\mathrm{e}^{-2B_2^{(2\mathrm{D})}N/A}. \quad \text{(S12)}$$

We now assume the adsorbing surface of the polymer as a cylinder with the area $A = 2\pi RL$, where R is the radius and L the length. We can thus relate the adsorbed solutes per area N/A to the adsorption coefficient Γ' as $N/A = \Gamma' c_0/2\pi R$. Furthermore, we take into account that the virial expansion is valid for $B_2^{(2\mathrm{D})}N/A \ll 1$, which allows us to expand the second exponential function in Eq. (S12) to the first order, which gives

$$\Gamma' = 2\pi R\delta \mathrm{e}^{-\epsilon/k_\mathrm{B}T}\left(1 + \frac{B_2^{(2\mathrm{D})}\Gamma'}{\pi R}\right). \quad \text{(S13)}$$

Comparing the last equation to the expression $\Gamma' = \Gamma'_0 + \Gamma'_1 c_0$, we obtain $\Gamma'_0 = 2\pi R\delta \mathrm{e}^{-\epsilon/k_\mathrm{B}T}$ for the leading order of the adsorption coefficient, and the first-order correction then follows as

$$\Gamma'_1 = -\frac{B_2^{(2\mathrm{D})}\Gamma_0'^2}{\pi R}. \quad \text{(S14)}$$

The above approach is based on several approximations that prevent us to quantitatively compare its predictions to the MD results. First, the effective radius of the cylinder is $R = 0.5$ nm, comparable to the size of the solutes, which makes the two-dimensional treatment of the gas not precise. Second, the above approach treats the adsorption of the solutes on the polymer in terms of a smooth potential well of depth ϵ. In reality, the binding potential is a collection of individual interacting sites and therefore highly non-uniform. Nevertheless, the derived equation (S14) offers important insights into qualitative understanding of the observed trends in adsorption from the simulations.

The cooperativity effects in the case of NB can be seen also visually from the snapshot in Fig. S5, which shows that the NB molecules tend to bind around already adsorbed molecules on the polymer.

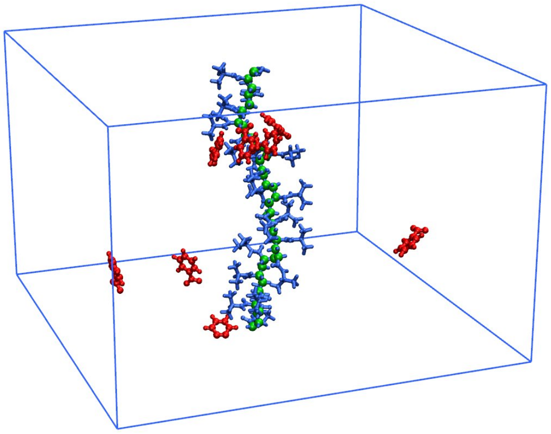

Figure S5: Simulation snapshot of a PNIPAM chain with the elongation $\lambda = 0.82$ and 8 NB molecules (shown in red) in the simulation box (water not shown), featuring a localized aggregation of four NB molecules at the same location on the PNIPAM chain.

References

(1) Ray, B.; Okamoto, Y.; Kamigaito, M.; Sawamoto, M.; ichi Seno, K.; Kanaoka, S.; Aoshima, S. Effect of Tacticity of Poly(N-isopropylacrylamide) on the Phase Separation Temperature of Its Aqueous Solutions. *Polym. J.* **2005**, *37*, 234–237.

(2) Jorgensen, W. L.; Tirado-Rives, J. The OPLS [optimized potentials for liquid simulations] potential functions for proteins, energy minimizations for crystals of cyclic peptides and crambin. *J. Am. Chem. Soc.* **1988**, *110*, 1657–1666.

(3) Frisch, M. J. et al. Gaussian 09 Revision E.01. Gaussian Inc. Wallingford CT 2009.

(4) Besler, B. H.; Merz, K. M.; Kollman, P. A. Atomic charges derived from semiempirical methods. *J. Comput. Chem.* **1990**, *11*, 431–439.

(5) Basma, M.; Sundara, S.; Çalgan, D.; Vernali, T.; Woods, R. J. Solvated ensemble averaging in the calculation of partial atomic charges. *J. Comp. Chem.* **2001**, *22*, 1125–1137.

(6) Tomasi, J.; Mennucci, B.; Cammi, R. Quantum mechanical continuum solvation models. *Chemical reviews* **2005**, *105*, 2999–3094.

(7) Fowler, R. H.; Guggenheim, E. A. *Statistical thermodynamics: a version of statistical mechanics for students of physics and chemistry*; University Press, 1952.